*Graphical Abstract

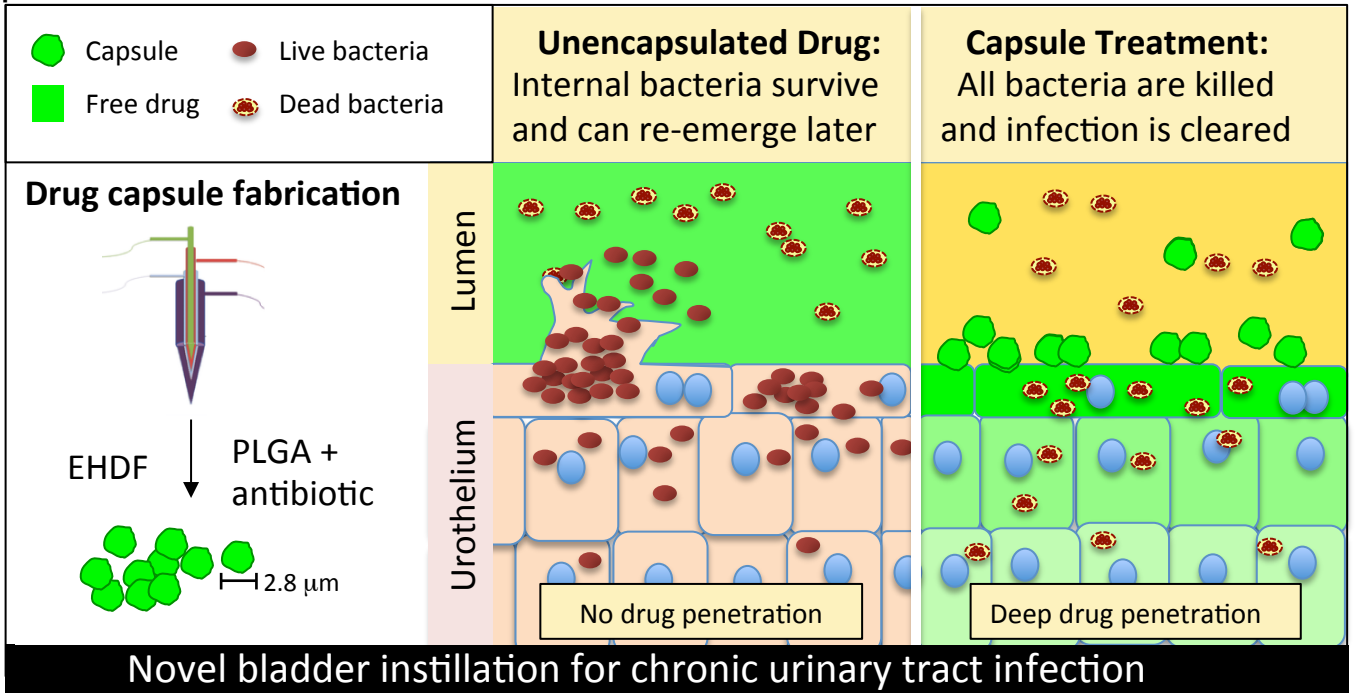

Novel Particles Conferring Eradication of Deep Tissue Bacterial Reservoirs for the Treatment of Chronic Urinary Tract Infection

Wai K. Lau[a,c], Dhanuson Dharmasena[a,b], Harry Horsley[b], Nazila V. Jafari[b], James Malone-Lee[b], Eleanor Stride[d], Mohan Edirisinghe[c] and Jennifer L. Rohn[b,*]

a. These two authors contributed equally to the work
b. Department of Renal Medicine, Division of Medicine, University College London, London, UK
c. Department of Mechanical Engineering, University College London, London, UK
d. The Institute of Biomedical Engineering, University of Oxford, Oxford, UK
* To whom correspondence should be addressed. j.rohn@ucl.ac.uk

Abstract

A significant proportion of urinary tract infection (UTI) patients experience recurrent episodes, due to deep tissue infection and treatment-resistant bacterial reservoirs. Direct bladder instillation of antibiotics has proved disappointing in treating UTI, likely due to the failure of infused antibiotics to penetrate the bladder epithelium and accumulate to high enough levels to kill intracellular bacteria. This work investigates the use of nitrofurantoin loaded poly(lactic-co-glycolic acid) (PLGA) particles to improve delivery to intracellular targets for the treatment of chronic UTI. Using electrohydrodynamic atomisation, we produced particles with an average diameter of 2.8 μm. In broth culture experiments, the biodegradable particles were effective against a number of UTI-relevant bacterial strains. Dye-loaded particles demonstrated that intracellular delivery was achieved in all cells in 2D cultures of a human bladder epithelial progenitor cell line in a dose-dependent manner, achieving far higher efficiency and concentration than equivalent quantities of free drug. Time-lapse video microscopy confirmed that delivery occurred within 30 minutes of administration, to 100% of cells. Moreover, the particles were able to deliver the drug to cells through multiple layers of a 3D human bladder organoid model causing minimal cell toxicity, displaying superior killing of bacterial reservoirs harboured within bladder cells compared with unencapsulated drug. The particles were also able to kill bacterial biofilms more effectively than the free drug. These results illustrate the potential for using antibiotic-loaded microparticles to effectively treat chronic UTIs. Such a delivery method could be extrapolated to other clinical indications where robust intracellular delivery is required, such as oncology and gene therapy.

Keywords: electrospray; urinary tract infection; 3D organoid; intracellular drug delivery; antimicrobial resistance

1. Introduction

The O'Neill report recently estimated that drug-resistant infections could cost the world USD $100 trillion in economic output and kill upwards of 10 million people per annum by 2050 if the rise of antimicrobial resistance (AMR) is not slowed [1]. Hence, there has been increasing interest in designing therapeutic strategies to minimise AMR. A disease in which AMR is of particular concern is urinary tract infection (UTI), which is one of the most common bacterial infections, affecting 150-200 million individuals annually. The associated financial burden is substantial, with healthcare expenditures and time away from work estimated to cost more than USD $6 billion globally per year [2-4]. Moreover, as UTI is the top infectious disease of the elderly, this burden will likely worsen as the global population ages [5].

The vast majority of UTIs affect the lower urinary tract and manifest as cystitis or urethritis. Whilst uncomplicated UTIs can be effectively treated with a short course of antibiotics, UTIs have a tendency to recur despite antibiotic treatment, with 20-30% of women with an acute UTI developing a recurrence within 6 months [3, 6]. UTIs related to catheter use is another area of great concern in healthcare-associated infections. In long-term care facilities, the source of over 50% of episodes of bacteraemia are related to catheter-acquired UTIs (CA-UTIs). The risk of bacteraemia in patients with indwelling catheters is 3-36 times that of patients without an indwelling catheter in long-term nursing homes [7]. Thus, the consequences of partially treated or untreated UTIs can be substantial and include frequent recurrences, ascending infection (pyelonephritis and sepsis), death, preterm birth and complications caused by frequent antimicrobial use such as *Clostridium difficile* colitis. There is also mounting evidence that low-grade, chronic infection can cause lower urinary tract symptoms such as overactive bladder, painful bladder syndrome, interstitial cystitis, and urinary incontinence, corresponding to an even higher estimated annual global cost of USD $76 billion [8-10].

Recurrence of UTI is thought to be facilitated by invasion of microorganisms into the apical urothelium of the bladder wall to take up residence within the cytoplasm of cells (11). Such bacterial reservoirs can then initiate longer-term intracellular colonisation of adjacent urothelial cells. While shielded from the host immune system and from antibiotics, which cannot penetrate or accumulate to high concentrations inside cells, such sequestered bacterial can persevere and subsequently emerge to initiate another episode of acute infection [11]. Although uropathogenic *Escherichia coli* is considered to be the most common cause of UTI, studies indicate that other important uropathogens involved with chronic infections, including *Enterococcus faecalis,* also have an intracellular phase [9, 12]. A recent paper on post-menopausal women with recurrent UTI revealed a remarkable spectrum of deep tissue residence by diverse different bacteria, including *E. faecalis*, in the bladder wall [13], which further highlights how difficult such infections are to treat with conventional antibiotics.

In addition, biofilms play a large part in UTI triggered by catheter use, and may also play a role in recurrent UTIs [14]. Bacterial "persister" subpopulations found within biofilms can become less metabolically active or dormant [15], enabling them to evade multiple antibacterial strategies, which almost always target actively metabolising bacteria [16]. All bacteria are thought to be capable of biofilm formation, and the presence of persister cells leads to the failure of antibiotic treatments and the emergence of antibiotic resistance in other systems [17].

Although strategies for the management of recurrent urinary tract infections (rUTI) are imperfect, daily prophylactic antibiotic use continues to be advocated although it is not curative [18]. Available oral drug therapies have not advanced significantly in recent years and difficulties surrounding drug compliance, systemic side effects and tolerance affect the clinician's ability to treat recurrent UTIs. Furthermore, UTIs have increasingly become harder to treat owing to the widespread emergence of an assortment of antibiotic resistance mechanisms [19, 20]. In one study, more than 9000 patient urine samples were tested for antibiotic resistance. The samples which contained uropathogens showed that over 20% were multi-drug resistant [21].

The drawbacks of oral antibiotics are intensified in the case of recurrent UTI, when long-term prophylactic doses are recommended [22], or in chronic UTI, where months of treatment may be required for symptom resolution [23]. The use of long-term oral antibiotics to treat chronic UTI can be inefficient due to failure to achieve the concentration of systemic drug needed to achieve a satisfactory dose within the bladder. The treatment duration can be hindered by patient compliance, antibiotic resistance, biofilm formation, ineffective regimes, systemic side effects and drug expense. Our local experience is that the oral treatment regime is not sufficient to treat all cases of chronic UTI. Thus, focusing on improving drug delivery is an important consideration in therapy development.

Although approaches targeting uropathogenic bacteria are being pursued, including vaccines and antivirulence therapies, the diversity among uropathogens poses significant challenges for these types of therapy, and antibiotics remain the most versatile strategy we have [24, 25]. A new delivery system for proven antibiotics would ideally achieve high drug concentrations in a confined and localised method and in a modality that allows the drug to penetrate through the urothelial cell membranes, and ideally biofilms, without influencing AMR in other bodily niches such as the gut.

Previous work has indicated that a combination of ultrasound and microbubbles can enhance drug penetration into cells and this has been applied successfully to the delivery of antibiotics [26]. A disadvantage of this approach for bladder applications, however, is the need to expose large regions of tissue to ultrasound, ideally using an extracorporeal probe. The aim of this study was to explore an alternative approach using polymeric microparticles as the delivery vehicle, which offer longer lifetimes than do microbubbles and do not require ultrasound to stimulate drug release to promote penetration. To this end, high doses of a common antibiotic (nitrofurantoin) were encapsulated within poly(lactic-co-glycolic acid) (PLGA) microparticles to produce a formulation suitable for direct infusion into the bladder by a routine clinical procedure (catheterisation). We utilised co-axial electrohydrodynamic atomisation (electrospraying) to prepare the particles, and characterised their morphology and release characteristics before assessing their therapeutic capacity in a human organoid model.

2. Methods

2.1 Electrohydrodynamic processing

In this process, liquid solutions flow through a metallic orifice under the effect of an electric field that directs the liquid streams into a fine jet. As the jet breaks up, near monodisperse particle formation occurs [27]. Particle size and morphology can be precisely controlled by adjusting various processing parameters [28]. Within a one-step process, a high encapsulation efficiency can be obtained with multiple component encapsulation. Electrospraying has been shown to be low cost, versatile and powerful. Using co-axial needles, multi-layered particles can be produced to specified dimensions (200 nm to 100 μm), with an excellent degree of uniformity (less than 1% variation in diameter) and dose control, at rates of ~ 10^{10} particles per minute per nozzle [29, 30].

PLGA (copolymer 50:50, Resomer RG503H) was purchased from Evonik Industries AG (Essen, Germany); acetone, fluorescein isothiocyanate (FITC) and nitrofurantoin were purchased from Sigma Aldrich (Poole, UK). PLGA was dissolved in acetone at 3 wt.%. Nitrofurantoin was dissolved in PLGA/acetone solution at 3.5 mg/ml and processed to make the active particle, called CapFuran, an identical lab-produced version of CapFuran®, a GMP-produced product the subject of International (PCT) Patent Application No. PCT/GB2019/050152. FITC was dissolved in nitrofurantoin/PLGA/acetone solution at 1 mg/ml and processed to make the tracer particle, called CapFuran-FITC. PLGA alone was used to make the negative control particle, called CapFuran-Placebo. Using a climate controlled custom-made setup, the solutions were pumped using a gas pressure-driven system at a constant flow rate of 10 ml/hr to a needle system. A potential difference of 17 kV was applied to the needle. The solutions were sprayed between 16 – 20 ˚C and 50 – 68 % relative humidity. After collection on a stainless-steel plate, the particles were transferred using a spatula to glass vials for storage and transport at ambient temperature (18 – 20 ˚C), measured using a data logger (Testo 174t).

2.2 Determination of particle morphology and size distribution

Samples were transferred onto a glass slide and imaged with optical and electron microscopy. Optical micrographs were taken with a camera (Micropublisher 3.3 RTV, 3.3 mega-pixel CCD Color-Bayer Mosaic, Real Time Viewing camera, Media Cybernetics, Marlow, UK) fixed to an optical microscope (Nikon Eclipse ME 600, Nikon, Japan). Samples on glass slides were gold-coated using an ion sputter coater (Quorum Q150R ES) for 90 seconds at 20 mA before scanning electron micrographs were taken using a scanning electron microscope (JEOL JSM-6301F or Hitachi S-3400N). Particle sizes were measured using the imaging software, ImageJ (NIH) [31].

2.3 Confirmation of chemical identity

Fourier Transform Infrared (FTIR) analysis was performed via Attenuated Total Reflection FTIR spectroscopy (ATR-FTIR) measurements (Bruker Vertex 90 spectrometer), and spectrographs were interpreted using OPUS Viewer version 6.5 software. The resolution was 4 cm^{-1} and the scan count was 16, over 4000-500 cm^{-1} at ambient temperature. Raman Spectroscopy was performed using a Renishaw-2000 laser Raman spectroscopy system at a wavelength of 785 nm with a Leica DMLM optical microscope and total exposure time of 10 seconds. GRAMS/32 software was used to measure Raman shifts.

2.4 Determination of loading capacity and encapsulation efficiency

To determine the loading capacity, 10 ml of acetone was added to 10 mg of CapFuran to fully dissolve both nitrofurantoin and PLGA. The resulting solution was then analysed using an ultraviolet/visible spectrophotometer (Jenway 6305 UV/Visible spectrophotometer, Bibby Scientific, Staffordshire, UK). The reading was compared against a calibration curve produced using samples of 0.5, 0.25 and 0.125 mg/ml of nitrofurantoin in acetone that were analysed on a UV spectroscope between 300-400 nm with a scan interval of 2 nm. The values at 370 nm were recorded and linear regression line drawn.

Loading capacity (%) was calculated using the following equation (1):

$$LC\ (\%) = m_d/m_p \qquad (1)$$

where m_d is the total mass of the drug in the sample determined as above and m_p is the total mass of the particles analysed.

Encapsulation efficiency (%) is calculated using the following equation (2):

$$EE\ (\%) = LC\ (\%)/\ LC_{Max}(\%) \qquad (2)$$

where LC_{Max} is the theoretical maximum loading capacity, determined as the ratio of the total mass of drug in the processed suspension and the total mass of particles analysed.

2.5 Particle reconstitution for experiments

All microparticle derivatives were initially resuspended in 0.9% normal saline (Baxter Healthcare Ltd, UK) at a concentration of 2 mg/ml in a glass vial at RT (except for Figure 3, where we resuspended the vials at 2.5 mg/ml to test higher concentrations). Because the drug nitrofurantoin is incorporated at 10% of the dry mass during the manufacturing process (c.f. section 3.2), 2 mg/ml is equivalent to 200 μg/ml of nitrofurantoin, which is the average expected concentration reached in the bladder following standard oral delivery according to the manufacturer's pharmacological information. The vial was capped and shaken vigorously for 20 seconds, and used within 5 minutes. When required, lower doses were achieved by further dilution in saline to the desired concentration. For experiments requiring CapFuran-Placebo or CapFuran-FITC the same reconstitution method was used. In the case of the latter, the quantity of dye incorporated was 0.7% of the dry mass as it was only present in the outer layer, corresponding to 14 μg/ml of free dye in solution.

2.6 *In vitro* drug release assay

The *in vitro* drug release profiles for nitrofurantoin-loaded microparticles were evaluated using the dialysis bag method. In brief, the dialysis bag (MWCO 12 KDa), containing 2 ml of reconstituted CapFuran, was put in a 250 ml beaker containing 98 ml of release medium (normal saline pH 7.4). The system was maintained at 37 °C with constant magnetic stirring (100 RPM) during the experiment. All experiments were carried out in triplicate. At predetermined time intervals, 1 ml of the external medium was withdrawn from the beaker

and sampled before replacing the solution back into the beaker to maintain constant volume. The sample was analysed by measuring the absorbance of nitrofurantoin using an ultraviolet-visible spectrophotometer (Jenway Genova Plus UV/Visible spectrophotometer, Bibby Scientific, Staffordshire, UK), before being returned to the beaker. Nitrofurantoin has two peaks when absorbance is measured using a spectrophotometer (370 nm and 266 nm). Estimations of drug concentrations were made by measuring absorbance at a wavelength of 370 nm.

2.7 Determination of antibacterial activity against various UTI bacteria over 24 hours

Antimicrobial killing assays in broth were each performed on four independent occasions using 5 different bacterial isolates: *E. coli* UTI89; *E. coli* ATCC 25922; a lab-passaged reference strain of *E. faecalis* ("EF-CIb") derived from bacteria isolated from a patient with chronic UTI [12] from the Whittington Hospital lower urinary tract symptoms clinic)*; E. faecalis* ATCC 29212; and *Staphylococcus aureus* ATCC 29213. *E. coli* strains were grown in Luria Broth (LB) media whilst the other strains were grown in Tryptic Soy Broth (TSB). Strains of each bacteria were grown in their respective media overnight on an orbital shaker (150 RPM) at 37 °C. 100 µl of overnight culture was re-suspended in 5 ml of fresh media solution (37 °C at 150 RPM) for 2-3 hours until an OD value of 0.4 was achieved (mid-log phase). The activities of pure nitrofurantoin (200 µg/ml), CapFuran (2 mg/ml), CapFuran-Placebo (2 mg/ml), and media solution alone were investigated. Once an OD value of 0.4 was achieved, antibiotics, particles or media solution were added to each T25 flask. Sampling was carried out at 0, 2, 6, and 24-hour time points. At the given time points, 100 µl of inoculum was withdrawn and ten-fold serial dilutions were plated onto TSA or LB agar plates in duplicates. The plates were incubated for 24 hours at 37 °C before colonies were counted. Because the negative control samples (CapFuran-Placebo and media alone) vastly outgrew the intervention samples, we capped the dilutions to be analysed at 10^{-9}, equivalent to an arbitrary cut-off of 10^{-12} cfu/ml in the negative control arms of the most highly growing cultures. The average of technical duplicates obtained from these 4 biologically independent experiments were used to generate the graphs as median with 95% CI.

2.8 Determination of extended antibacterial activity against *E. faecalis*

The protocol for the extended antibacterial assay was similar to that previously reported [32]. Briefly, an overnight culture of *E. faecalis* clinical strain "EF36" (isolated directly from a patient with chronic UTI [12], in TSB was adjusted to the equivalent of a 0.5 McFarland standard using CnT Prime bladder epithelial media (CELLnTEC, Switzerland). The solution was further diluted 1:250 in the same media and added to the particles and drug solutions in 15 ml Falcon tubes. The tubes were incubated overnight (16-24 hours) in darkened conditions at 37 °C with loose caps to allow aerobic respiration before plating on CPS Elite agar plate (bioMerieux, Hampshire UK) overnight at 37 °C for enumeration. Colonies were recorded by counting and back-calculating the total amount of viable "colony-forming units" (CFU) in the original solution, taking into account a ten-fold dilution series out to 10^{-3} . To help facilitate the measurement of bacteria, if the quadrant contained too many colonies to count individually the count was arbitrarily estimated at 600 CFU, and a quadrant growing a seamless lawn of bacteria, indicating saturation, was set at 1000, as described previously [32]. At this saturation point, further dilutions were not employed. Six independent biological replicates were performed, and the mean and standard error of the mean were plotted.

2.9 Cell culture

HBLAK (CELLnTEC) is a commercially available spontaneously immortalised human bladder epithelial progenitor cell line which has not undergone transformation, which was derived from the trigone region of a healthy male bladder. As such, HBLAK cells retain many features of their primary cell counterparts, including the ability to stratify and differentiate into umbrella cells, the cell type that uropathogens encounter in the bladder lumen [33]. HBLAK cells were used up to passage 40. Cells were passaged and maintained as described previously [33]. To create 2D monolayer cell culture models, 8-well glass chamber slides (Nunc Lab-Tek II, Sigma-Aldrich) were pre-treated with 200 µl of calcium- and magnesium-free phosphate buffered saline (PBS, Sigma-Aldrich) supplemented with 0.5% fibronectin from bovine plasma (Sigma-Aldrich) and incubated at 37 °C in 5% CO_2 for one hour. The solution was aspirated and 1x 10^5 cells/ml were placed into each well of the chamber slide. Cells were evaluated microscopically to ensure a confluent monolayer of cells had formed before experiments commenced.

The creation of three-dimensional stratified human bladder organoids has been described previously [33]. Briefly, HBLAK cells were seeded onto transwells and grown to 100% confluency. Next, the basal and apical medium was removed and replaced with low BPE, calcium-rich (1.2mM) 3D differentiation barrier medium (CnT Prime 3D, CELLnTEC) for 24 hours to encourage differentiation, and then the apical chamber was replaced with pooled, filter-sterilized human urine from healthy male and female staff volunteers. Basal medium and apical urine were replaced every three days and the culture incubated for 14-16 days at 37 °C in 5% CO_2.

2.10 Determination of intracellular delivery of cargo

HBLAK cells growing as 2D monolayers on 8-well glass chamber slides were treated with particles loaded with the fluorescent dye FITC (Capfuran-FITC); or with the concentration of unencapsulated free FITC equivalent to that harboured in the particles, for the doses and times indicated in Figure 2. Specifically, cell culture medium was removed from each well and replaced with 200 µl of fresh medium. Then, 200 µl of particle or dye solution at twice the required final concentration was added to the same well for a total volume of 400 µl and a dilution of 1:2. Cells were incubated under normal culture conditions for the specified times. After treatment, cells were washed gently with PBS before fixing cells with 4% formaldehyde in PBS for 20 minutes and permeabilising their membranes in 0.2% Triton-X100 (Sigma-Aldrich) in PBS for 5 minutes at room temperature (RT) followed by a single wash with PBS. The cells were then stained with 4'',6-diamidino-2- phenylindole, (DAPI, 1 µg/µl; Sigma-Aldrich) in PBS for 1 hour at RT to visualize DNA. The staining solutions were gently aspirated and the cells washed 4 times in PBS before mounting. The slide wells and gaskets were carefully removed prior to the addition of FluorSave reagent (Calbiochem) and a coverslip fixed in place with clear nail varnish.

The experiments were repeated on the bladder organoids to determine uptake in three-dimensional tissue. The cells were treated with either particles loaded with the fluorescent green dye FITC (CapFuran-FITC), the equivalent dose of free FITC in media solution or, as a control, CnT differentiation barrier media (CnT-Prime-3D, CELLnTEC) for 2 hours at 37 °C in 5% CO_2. The filter inserts were transferred into new 12-well plates and submerged in 4% methanol-free formaldehyde (Thermo Fisher Scientific, UK) in PBS overnight at 4 °C. After fixation, the inserts were stained as above but with the addition of phalloidin conjugated to

AlexaFluor-633 (0.6 µg/ml) to stain filamentous actin (Sigma-Aldrich, UK). The inserts were then washed four times before mounting on glass slides as above. Static imaging on fixed preparations was carried out using epi-fluorescence microscopy on an Olympus CX-41 upright microscope, and confocal laser scanning microscopy (CLSM) on Leica SP5 and SP2 microscopes. Images were processed and analysed using Infinity Capture and Analyze V6.2.0, ImageJ 1.50h 50 [31] and the Leica Application Suite, Advanced Fluorescence 3.1.0 build 8587 Software, respectively. Live cell static imaging and timelapse videomicroscopy of live cells was performed by growing cells to confluency on 35mm live-imaging dishes (µ-Dish, Ibidi, Germany) inside a stage-top incubator receiving 0.35 l/min of pre-mixed gas containing 5% CO_2 within a fully-enclosed microscope cabinet heated to 37 °C. To stain the cell nucleus, living cells were treated at a concentration of 1 µg/ml Hoechst 33342 (ThermoFisher Scientific) in media for 15 minutes before imaging. Images were taken using a fully-motorised Leica SP8 laser scanning confocal microscope equipped with hybrid detectors and hardware-based autofocus. Leica Application Suite X (LASX, version 3.5.2.18963, with Lightning super-resolution module) was used to control the microscope and analyze data. Live Z-stacks comprising of 10 slices (Z-step of 1.93 µm) at 16bit at a resolution of 2880 X 2880 were taken every 90 seconds for a total duration of 30 minutes.

2.11 Enumeration of intracellular bacteria (antibiotic protection assay)

HBLAK cells ($2x10^5$ cells) were seeded onto 12 mm diameter 0.4 µm thick polycarbonate filter inserts (two per treatment) and organoids were grown as described above. A colony of *E. faecalis* EFCIb was added to 5 ml of TSB (grown overnight in an orbital shaker at 37 °C). 100 µl of bacteria were resuspended in 5 ml of fresh TSB for 3 hours and an optical density (OD_{600}) corresponding to 0.4 ($2x10^9$ CFU) was used. For infection, 500 µl of CNT 3D Prime media and bacteria were added to the inserts at a multiplicity of infection (MOI) of 10, and the cells were incubated at 37 °C in 5% CO_2 and left overnight. After washing with PBS solution once, inserts were treated for 2 hours with gentamicin (150 µg/ml, Sigma-Aldrich, UK) and vancomycin (10 µg/ml, Sigma-Aldrich, UK) in CNT 3D Prime media solution. The killing of extracellular bacteria with gentamicin and vancomycin was confirmed by plating the supernatant prior to exposure to the therapy. The inserts were washed once with PBS (supernatants were plated as above) and assigned treatment with 2 mg/ml CapFuran; 2 mg/ml CapFuran-Placebo; 200 µg/ml nitrofurantoin; or CNT 3D Prime media solution ("mock") for 2 hours. The cells were washed thoroughly with PBS before lysing with 1% Triton-X100 and plated as above. This level of detergent does not affect bacterial viability appreciably. To establish the correct CFU (colony forming units) per ml, the mean bacterial counts from the duplicate samples were adjusted to take into account the serial dilution. The experiment was repeated two more times (total N=3).

2.12 Biofilm assay

A colony of *E. faecalis* EFCIb was added to 5 ml of TSB (and grown overnight in an orbital shaker at 37 °C). A 1:250 solution of bacteria supplemented with fresh TSB and 1% glucose (Sigma-Aldrich, UK) was transferred into 96 well plates. Biofilms were allowed to form by incubating the plates in a humidified chamber at 37 °C for 48 hours in an orbital shaker (150RPM). After 48 hours, the supernatant solution was aspirated and plates were washed with sterile PBS, leaving behind the biofilm. Biofilm formation on parallel control wells was confirmed with crystal violet staining (data not shown) before either treating the wells with 2 mg/ml CapFuran; 2 mg/ml CapFuran-Placebo; fresh TSB only; or 200 µg/ml unencapsulated nitrofurantoin, all resuspended in TSB solution with a total volume of 100 µl. After overnight

treatment allowing the capsules in liquid media to interact with the biofilm formed on the substrate, the supernatants were discarded and the plates washed gently four times with PBS. Next, the biofilms were mechanically disrupted using a pipette tip to liberate any remaining viable bacteria. Biofilm killing was quantified in duplicate by spot-plating and enumeration on TSA plates. The whole biofilm experiment was repeated two additional times (total N=3).

2.13 Cytotoxicity assay

A colorimetric Lactate Dehydrogenase (LDH) assay kit (Thermo Scientific) was used to measure potential cell damage from CapFuran or nitrofurantoin. The procedure was carried out as previously described and as directed by the manufacturer [34, 35]. HBLAK-derived bladder organoids were grown for 14 days as detailed above. The bladder organoids were then exposed to 1 ml of culture media (control) or 1 ml of culture media containing CapFuran 1 mg/ml; CapFuran 2 mg/ml; 100µg/ml unencapsulated nitrofurantoin; 200 µg/ml nitrofurantoin; 100 µl of 10X lysis buffer (maximum LDH control); or culture medium containing 10% ultra-pure water (to measure spontaneous LDH release). Experiments were carried out in triplicate. All organoids were subsequently incubated for 60 minutes at 37 ^{o}C in 5% CO_2. After incubation, 50 µl of medium from the apical chamber of each treated organoid was transferred to 3 wells of a flat-bottomed 96-well plate (Corning). 50 µl of reaction buffer (lactate, NAD^+, tetrazolium salt (INT)) was then added to each well and gently mixed before incubating the plate at room temperature for 30 minutes in the dark. The reaction was then halted by adding 50 µl of 'stop solution' (0.16M sulfuric acid) to each well. The experiment was repeated five more times (total N=6). To quantify the amount of LDH released, the 96-well plate was analysed by a colorimetric spectrophotometer (Biochrom EZ Read 400) at an absorbance of 492 nm and 650 nm. Microsoft Excel was used to subtract the background reading from the LDH reading before calculating cytotoxicity in % using the following equation (3):

$$\% \text{ Cytotoxicity} = \frac{\text{Treatment associated LDH release} - \text{Spontaneous LDH release}}{\text{Maximum LDH activity} - \text{Spontaneous LDH release}} \times 100 \quad (3)$$

2.14 Statistical analysis

Data were analysed using IBM SPSS Statistics version 25 (or GraphPad Prism version 7 in the case of Figure 2), with the specific tests used indicated in the Results and Discussion section (3) as they are referred to.

For Figure 3 graphs, a non-parametric, Kruskall-Wallis one-way analysis of variance was deployed for each dataset (in the case of Figure 3a, a log scale was used to enable better visualisation and, therefore, easier comparisons). The results from these tests, as with a parametric ANOVA test, indicates that a statistically significant difference exists between some or all of the groups. 95% confidence intervals were constructed around the median for each group to allow the reader to observe where these differences lie. Further post hoc testing was not deemed appropriate due to the likelihood of type-II error and statistical power.

3. Results and Discussion

3.1 Particle characteristics

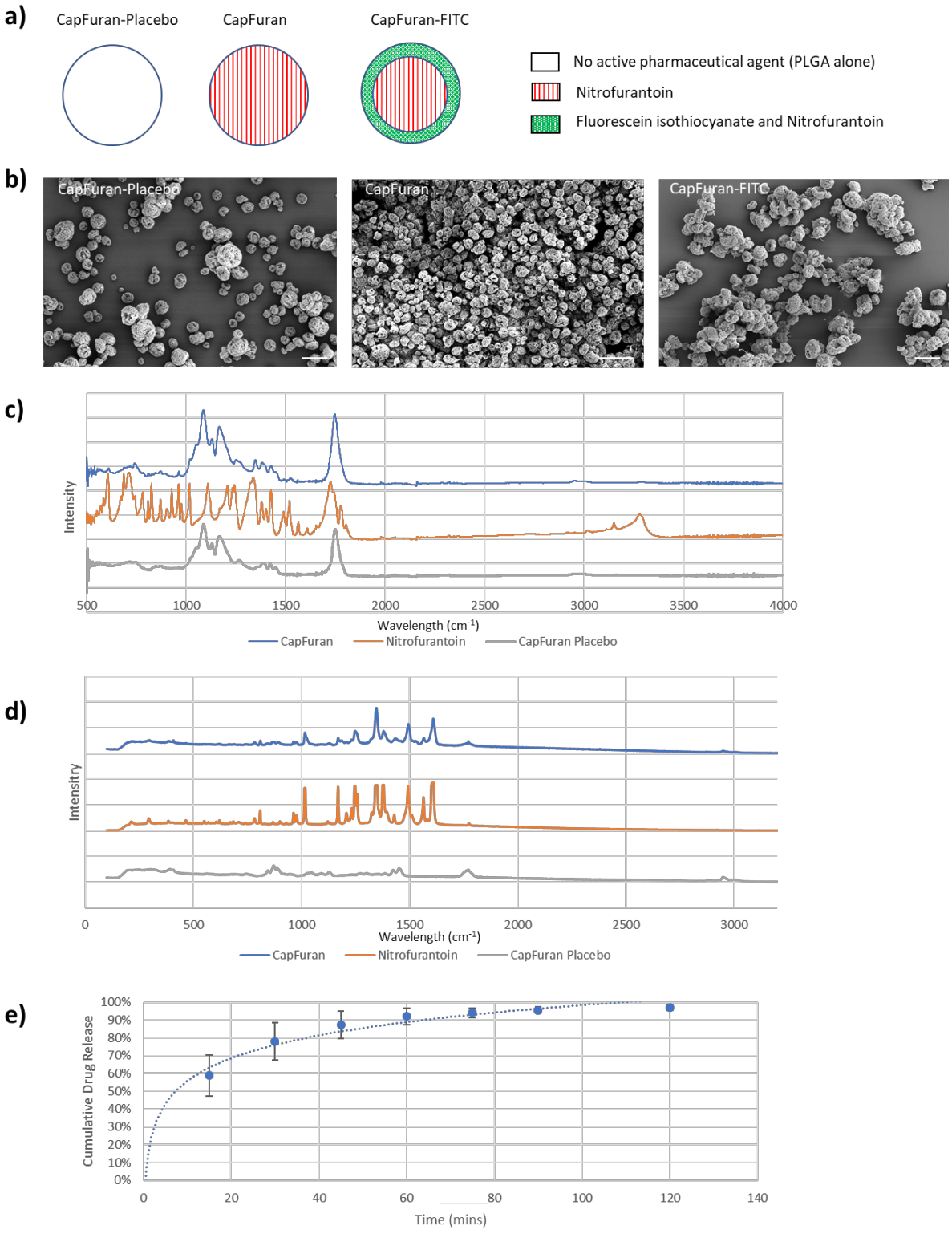

Figure 1: Physical and chemical characteristics of the particles. **a)** A schematic diagram of the three particle formulations that were produced. **b)** Scanning electron microscopy (SEM) images of left: CapFuran-Placebo, middle: CapFuran, and right: CapFuran-FITC. Images were taken at 1000x magnification; Scale bar is 10 µm. **c)** Fourier Transformed Infrared (FTIR) spectra and **d)** Raman spectra of CapFuran, free nitrofurantoin and CapFuran-Placebo. **e)** Drug release curve of CapFuran at 2.5mg/ml. Means are plotted, and error bars indicate 95% confidence intervals; n= 3.

We investigated the morphology of all three PLGA particles (see **Figure 1a** for a schematic) using SEM. **Figure 1b** shows that all particles were approximately spherical with a porous surface. The average diameter of CapFuran was 2.8 ± 1.4 μm (*n* = 389, where *n* is the number of particles measured), and the two control particles (CapFuran-Placebo and CapFuran-FITC) had diameters of 4.1 ± 1.2 μm and 3.4 ± 1.0 μm respectively.

The FTIR spectrum of CapFuran was similar to that of CapFuran-Placebo (**Figure 1c**). The major peaks occurred at approximately 1750 cm^{-1}, corresponding to the C=O carbonyl group; 1350-1420 cm^{-1}, corresponding to the C-H methyl groups and 1080; and 1120 and 1170 cm^{-1}, corresponding to the C-O-C ester bonds. The intense peaks seen in the spectrum of nitrofurantoin were also apparent in the CapFuran FTIR spectrum, although with lower intensity due to a masking effect of the more prominent polymer peaks, confirming the chemically unchanged presence of nitrofurantoin in CapFuran.

Figure 1d shows the Raman spectra of CapFuran, CapFuran-Placebo and free nitrofurantoin. The majority of the peaks seen with nitrofurantoin were also seen in CapFuran with some key differences, in contrast to the FTIR spectrum. The C-H peaks seen at around 2950 cm^{-1} in PLGA were absent in nitrofurantoin but present in the CapFuran spectrum. Three distinct peaks seen in the 800-900 cm^{-1} range for nitrofurantoin were not seen or may have been masked in the CapFuran spectum. The relative intensity of the twin peaks seen at 1350 and 1380 cm^{-1} were altered in the CapFuran spectrum, with the later peak at 1380 cm^{-1} much less intense relative to the former 1350 cm^{-1} peak.

Taken together, the FTIR and Raman spectra of nitrofurantoin-loaded PLGA particles displayed characteristic peaks of both polymer and drug with no major shift or loss of functional peaks. The spectral study thus suggests that there were no significant molecular interaction between PLGA, nitrofurantoin and the solvent during processing that would alter the chemical structure of the drug or polymer.

3.2 Loading capacity, encapsulation efficiency and drug release rate

The loading capacity was calculated as 9.8% w/w and the total maximum loading capacity as 10.4%, resulting in an encapsulation efficiency of 94%. This high encapsulation efficiency is typical of the electrospraying process and represents one distinct advantage of this manufacturing technique [36]. The loading capacity was approximated to 10% for this study. As a result, when comparing to a therapeutic dose of 200 μg/ml of free drug, we used 2 mg/ml of particles.

We used a conventional dialysis bag method to determine the drug release kinetics. The results are shown in **Figure 1e**. The curves demonstrate CapFuran releasing over 50% of the encapsulated drug within the first 15 minutes. By 60 minutes approximately 90% of the drug had been released. This pattern is consistent with a simple diffusive release from the polymeric matrix, which is rapid due to the porosity of the particles.

3.3 CapFuran can kill various bacterial strains more effectively than can the free drug

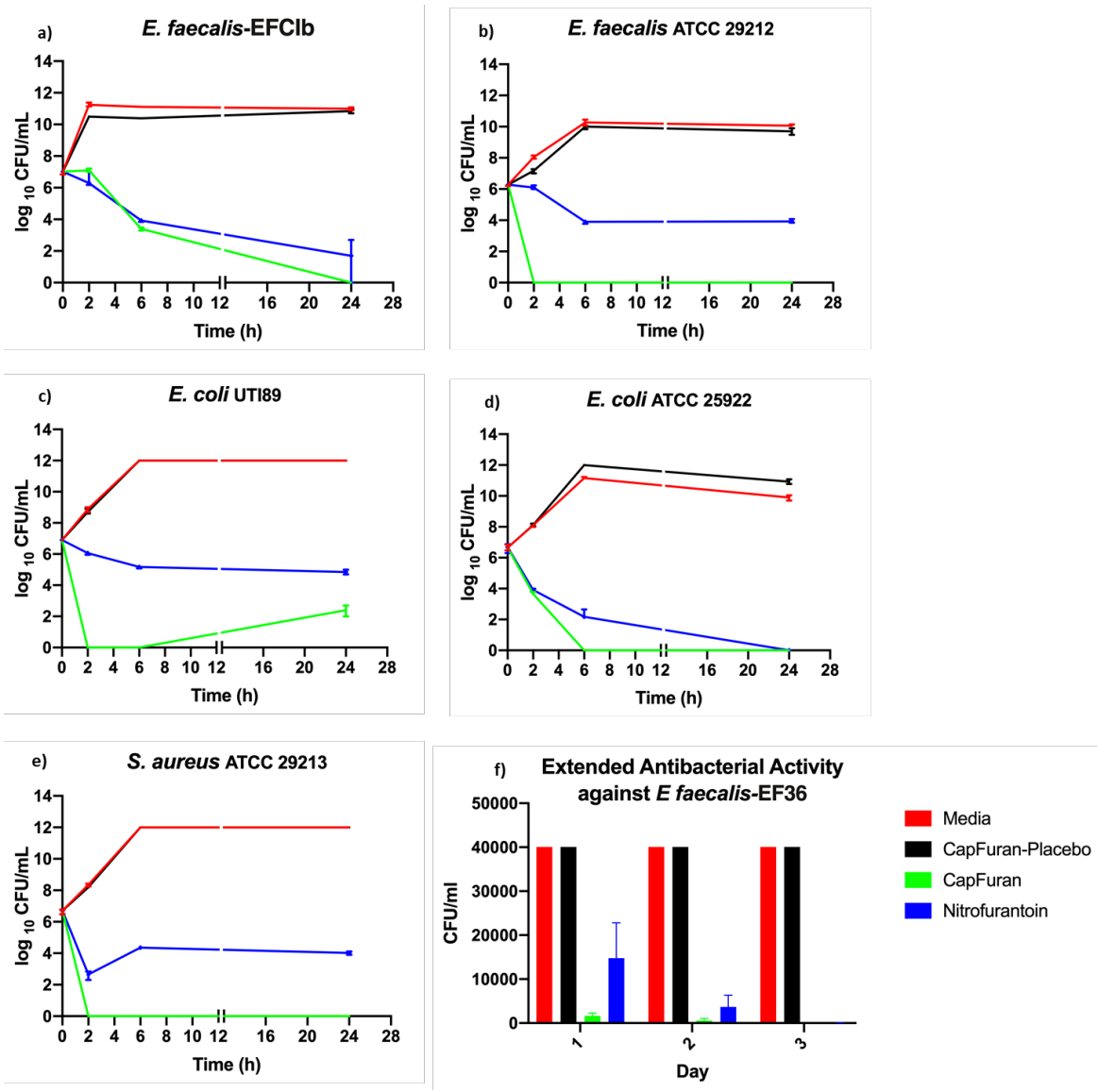

Figure 2: Efficacy of CapFuran against various bacterial strains.
a-e) Antimicrobial time kill assays were carried out to determine the bactericidal activity of CapFuran (2 mg/ml), CapFuran-Placebo (2 mg/ml), free nitrofurantoin (200 μg/ml) and media only (equivalent volume) on the indicated bacterial strains; $\log_{10}$ colony-forming units (CFU)/ml are shown on the y-axis and time (hours) on the x-axis. The concentration of free nitrofurantoin (200 μg/ml) was equivalent to the amount of drug in CapFuran; the median of 4 independent experiments is shown; bars indicate 95% confidence intervals of median values. The y-axis is cut after 12 hours to indicate longer time intervals thereafter. **f)** Antibacterial activity against direct clinical isolate *E. faecalis*-**EF36** after being subjected to various treatments (see above) in shaking broth culture over a total duration of 3 days. Cultures that became saturated (defined as a bacterial lawn at the highest dilution) were given an arbitrary cut-off value – see Methods for details. For this graph, the mean of 6 independent experiments is shown; bars indicate standard error of the mean (SEM).

To assess the suitability of CapFuran as an antimicrobial therapy, we first examined its ability to kill bacteria at various time points post-treatment in shaking broth culture. **Figure 2a-e** show the results of the antimicrobial assay experiments using five different isolates of bacteria commonly implicated in chronic UTI. These included two strains of *E. faecalis*

(Figure 2a and b), two strains of *E. coli* **(Figure 2c and d),** and a strain of *S. aureus* **(Figure 2e)**.

In a time-course assay, CapFuran proved to be superior compared with free drug against two of the strains, including *E. faecalis* 29212, and UTI89, the strain of *E. coli* most commonly studied to model UTI virulence, albeit with different kinetics (**Figure 2a-e**). Specifically, bacterial growth was completely suppressed by CapFuran, but not free drug, after two hours in the case of *E. faecalis* ATCC 29212 (as assessed by two-way ANOVA with Tukey's multiple comparisons test, $p < 0.0114$). The same dose of CapFuran suppressed the growth of *E. coli* UTI89, a well-known uropathogenic strain, after two hours, and though this was not sustained over the 24-hour period, it was superior to free drug ($p < 0.0029$ at two hours). CapFuran killed *E. coli* (ATCC 25922) completely by 6 hours, and the *E. faecalis* clinical reference strain EFCIb, by 24 hours, approximately equivalent to the performance of the free drug alone. In these experiments, although it was interesting to see that the encapsulation could provide enhanced antimicrobial activity in some cases, we were only looking to demonstrate that the encapsulation did not impair nitrofurantoin's killing ability. Further studies are required to elucidate the underlying mechanisms. Encapsulation may provide an advantage over free drug by increasing the local concentration of drug adjacent to a cell; it is yet to be established, however, whether the surface characteristics of the CapFuran particles also enhanced bacterial uptake of the drug.

In summary, CapFuran inhibited all species tested at least equally to unencapsulated nitrofuran, including pathogenic patient strains, and in some instances performed better. We also achieved efficient killing of other uropathogens, including *Klebsiella*, *Citrobacter* and *Enterobacter* (data not shown). These results are important, as in the case of chronic UTI, patients can harbour a range of infective species and usually more than one organism at a time [9]. *E. coli* is the most common species involved in acute community-acquired UTI in healthy young women [37], while *E. faecalis* is common in the elderly [9] and prevalent in hospital acquired- and catheter-associated UTI [38].

3.4 CapFuran effectively kills *E. faecalis*, a key pathogen in chronic UTI

E. faecalis, as mentioned above, is a particular problem in chronic UTI amongst the elderly, and is difficult to kill with conventional antibiotics because it forms protective intracellular reservoirs [12] that antibiotics cannot access well by free diffusion. Therefore, we wanted to confirm the effect of CapFuran in more detail on this particular bacterial species. **Figure 2f** shows antibacterial activity against a strain *E. faecalis* ("EF36", which was directly isolated from a patient with chronic UTI), after being subjected to various treatments in broth culture extended over a total duration of 3 days. Average numbers of bacteria throughout day 1 to day 3 were lower (but not statistically significantly) in the CapFuran group when compared with the nitrofurantoin group. The effect of CapFuran persisted from day 1 to day 3 as can be seen by the reducing mean bacterial count. CapFuran was statistically significantly superior to CapFuran-Placebo at all three timepoints (as assessed by two-way ANOVA with Tukey's multiple comparisons test, $p < 0.0001$ for all three). These experiments further confirm that encapsulation does not impair nitrofurantoin's basic ability to kill this important chronic uropathogen in a cell-free system. We hypothesised, however, that encapsulation could provide a distinct advantage over free drug when tested against bacteria that are sequestered within host cells, as occurs in chronic UTI. This is because free nitrofurantoin is generally impermeant and moreover is unlikely to penetrate and/or accumulate to therapeutic levels within bladder cells, which present a formidable barrier that protects the urothelium from the

toxic effects of urine [39]. Thus in subsequent experiments we set out to test how CapFuran performed in regards to cell penetration and intracellular bacterial killing.

3.5 CapFuran-FITC delivers cargo in a dose-responsive manner to cultured human bladder cells without apparent toxicity

A fluorescently labelled version of CapFuran (CapFuran-FITC) was used to assess intracellular delivery within a monolayer of human bladder cells (HBLAK). As shown in **Figure 3a**, 100% of cells took up the FITC dye after 2 hours of treatment at doses of 2.5mg/ml (equivalent to 17.5 μg/ml of dye, as the dye is 0.7% of the particle mass). As the dose decreased, the number of cells exhibiting fluorescence decreased, showing that delivery is cell-targeted and not merely reflecting general uptake via free diffusion of FITC that might have been released into solution prior to intracellular uptake. If uptake were due to free FITC diffusion into cells, all cells would be expected to display green fluorescence with a decrease in intensity accompanying a reduction in dose. Indeed, as shown in **Figure 3b**, free FITC at the equivalent of the highest particle dose (17.5 μg/ml) bestows a faint green staining to all cells but does not confer the bright green staining produced by delivery via CapFuran-FITC, and this staining decreases in all cells as the dose is reduced. No apparent toxicity was noted after CapFuran-FITC treatment; all cells appeared morphologically healthy by microscopy. **Figure 3c** shows a super-resolution image of living HBLAK cells having taken up the green cargo after 2 hours of treatment with CapFuran-FITC 2 mg/ml); note the dye is present in both the cytoplasm and nucleus as expected due to its size.

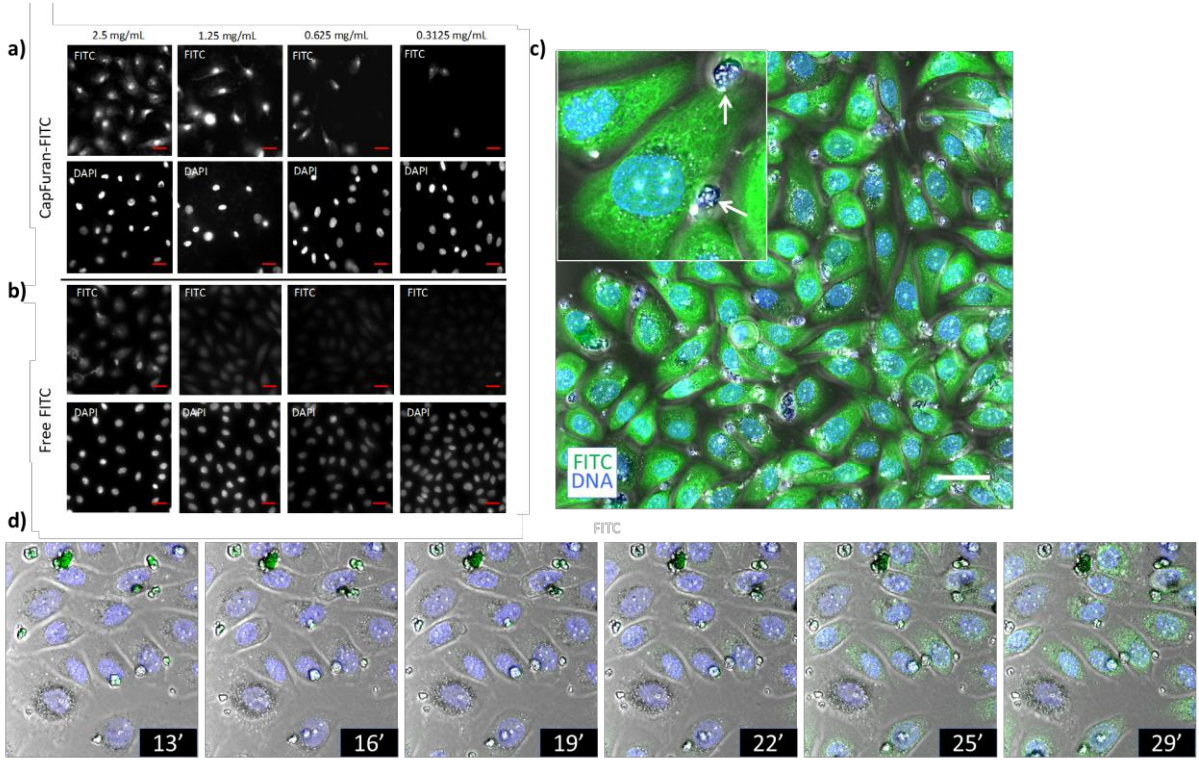

Figure 3: Ability of CapFuran to penetrate 2D bladder cell monolayers.
a) Cells were incubated with either CapFuran-FITC or the equivalent dose of free FITC on 2D monolayers for 2 hours. The concentrations of CapFuran used are noted on the top of the figure and contained respectively 10% and 0.7% of drug and dye by mass. Greyscale images of individual channels (FITC and DAPI, which stains the cell nucleus) are shown. There was dose-dependent specific delivery of CapFuran-FITC dye into the cells. **b)**

Comparison with equivalent amounts of free FITC is shown (from left to right, 17.5 μg/ml; 8.75 μg/ml; 4.38 μg/ml; 2.19 μg/ml). Scale bar for a) and b), 20 μm. **c)** Distribution of FITC cargo during cell delivery, showing 100% delivery. CapFuran-FITC (2 mg/ml) incubated for 2 hours on a monolayer of HBLAK cells were imaged live using super-resolution confocal microscopy. Scale bar, 20 μm. Hoechst (blue) was used to stain cell nuclei and FITC is shown in green. Inset shows an enlarged subsection; arrows indicate CapFuran particles. **d)** Timelapse video microscopy of live HBLAK cells treated with CapFuran-FITC (2 mg/ml); various still images are shown. Timestamps in minutes post treatment are indicated on each still image. (See **Supplementary Figure 1** for the full video).

To explore the kinetics of drug delivery in the context of target cells, we performed live timelapse imaging on monolayers of HBLAK cells immediately after addition of 2 mg/ml CapFuran-FITC. As shown in **Figure 3d (**and video in **Supplementary Figure 1)**, particles released cargo into cells by approximately 30 minutes without apparently being taken up themselves; all cells received cargo at approximately the same time. These results show that although in a cell-free system the cargo is gradually released over 90 minutes (**Figure 1e**), when in the presence of recipient cells, the delivery occurs far more quickly and simultaneously (with a good delivery profile by approximately 30 minutes). The underlying mechanisms are still under investigation.

Taken together, this set of experiments suggests that CapFuran-FITC can deliver cargo intracellularly extremely efficiently (all cells in the field of view showed uptake), and appears to achieve an intracellular concentration much greater that that conferred by free diffusion. The fact that the polymeric shell is not taken up by cells can be seen as an advantage, as incorporation of such a large structure might be expected to disrupt cell function. Instead, during clinical application, the residual extracellular shells would be expected to be expelled by urination, or safely biodegraded if not.

3.6 CapFuran-FITC can infiltrate a three-dimensional human bladder urothelial organoid model through multiple layers of cells whereas free FITC cannot

As UTI involves intracellular bacterial reservoirs within a stratified urothelium [11, 12], possibly including those embedded more deeply than just the surface cell layer [40], we wanted to assess penetration and bacterial killing in a more sophisticated model. Because rodents do not acquire UTI naturally, and significant differences exist between the rodent and human bladder [41], such as a thinner urothelium and different biomarkers [42], we used a human urothelial organoid model in preference to a mouse model. This organoid has been used to study UTI and was shown to respond in a manner reminiscent of what has been seen in patients [33]. In contrast to human cell monolayers, the organoid also presents a more formidable barrier to entry, since it elaborates uroplakin proteins and an apical extracellular mucosal glycosaminoglycan (GAG) layer [33].

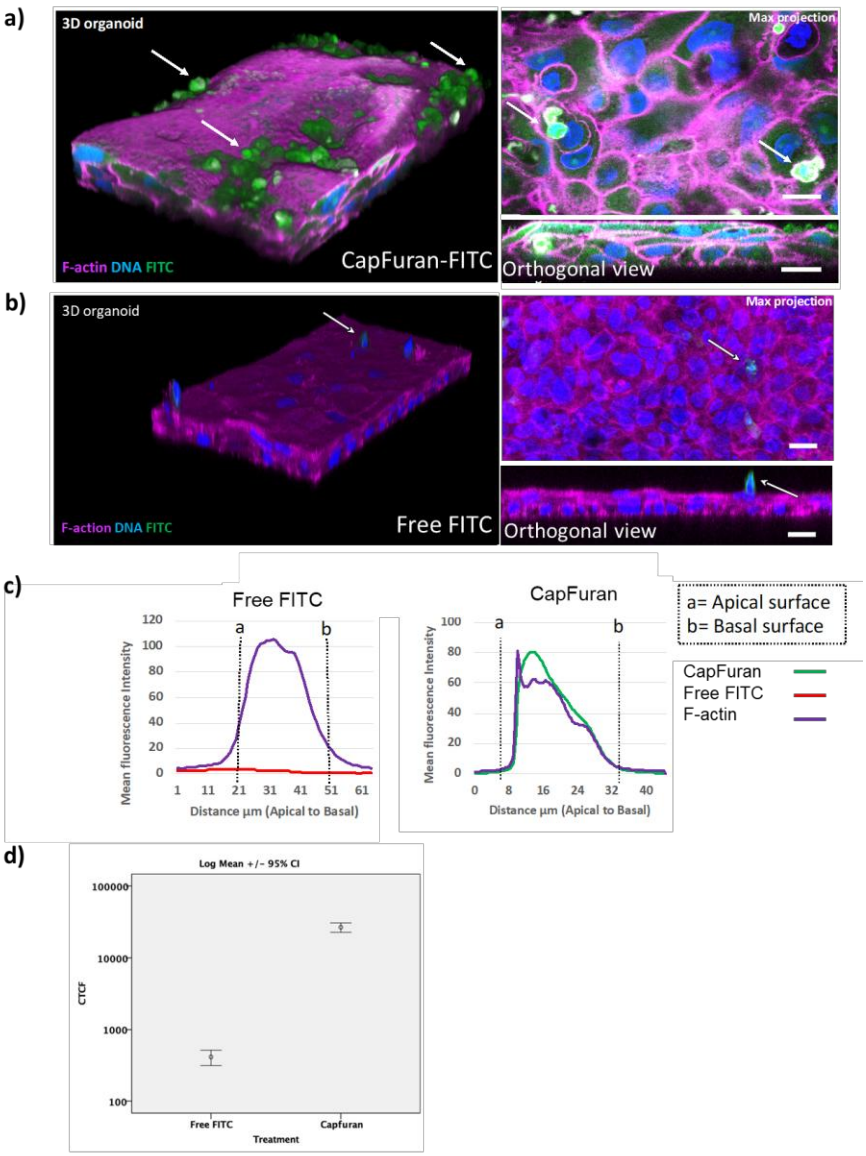

Figure 4: Penetration of CapFuran-FITC into a three-dimensional human urothelial organoid model. **a)** Urothelial organoid treated with CapFuran-FITC (2 mg/ml containing the equivalent of 14 µg/ml of dye). Image on left shows a confocal 3D reconstruction of the urothelial organoid which has been incubated with CapFuran-FITC (green) for 2 hours and stained with DAPI (stains DNA, blue) and phalloidin (stains filamentous actin, magenta). A maximum projection image (top right) and orthogonal view/sideview (bottom right) are also shown. White arrows show CapFuran-FITC particles. Scale bar, 10 µm. **b)** Organoid treated with equivalent dose of free FITC (14 µg/ml) for 2 hours and stained and presented as in (a). There is no apparent penetration of FITC inside the organoid model; free FITC (green) permeated dead surface cells only (white arrows). Scale bar, 10 µm. **c)** Z-axis profile plots of the urothelial organoids presented in (a) and (b) showing FITC penetration as a function of spatial location within the stratified urothelium. Mean fluorescence intensity of FITC and F-actin channels are plotted as a function of position on the apical-basal axis, confirming negligible penetration by free FITC. **d)** Data shown in (c) analyzed using corrected total cellular fluorescence (CTCF) statistical analysis. Image shows log mean CTCF and 95% confidence intervals.

As shown in **Figure 4a**, after treatment of the human organoid with 2 mg/ml of CapFuran-FITC (containing the equivalent of 14 µg/ml dye) for two hours (left image), the green dye is distributed in all cells (top right) through multiple layers of the stratified epithelium (cross-section, bottom right), indicating robust penetrative delivery of cargo. In contrast, when the organoid was treated with an equivalent amount of unencapsulated FITC (14 µg/ml; **Figure 4b**), no fluorescence was observed anywhere in the organoid, with the exception of a single

dead fluorescing cell protruding from the organoid (arrows); dead cells are known to take up this dye readily. No fluorescence was observed either in organoids treated only with control medium (data not shown). Z-axis profile plots (**Figure 4c**) were used to quantify the phenomena seen in **Figure 4a** based on the relative spatial position of pixels corresponding to green fluorescence with respect to pixels corresponding to phalloidin (magenta), which stains the F-actin cytoskeleton throughout the cell. When treated with CapFuran, profile plots confirm that FITC was present throughout the urothelial organoid with the highest amount in the apical cell layer, decreasing in intensity towards the basal layer of cells. When treated with free FITC, there was negligible to no FITC seen overlapping with the F-actin signal, indicating a failure to penetrate or accumulate. Note that this latter result supports the idea that the organoid presents a more formidable and physiological barrier, as dye cargo was able to penetrate monolayers to some extent, albeit inefficiently (**Figure 3b**). A quantitative analysis of the data shown in **Figure 4c** is shown in **Figure 4d**. The graph shows the log mean of the corrected total cellular fluorescence (CTCF) and 95% confidence intervals. These experiments show that cargo delivery is highly efficient in a more tissue-like human model and that delivery can occur to layers below the superficial layer of umbrella cells. This finding is promising because effective treatment of chronic UTI will require intracellular delivery and penetration to eradicate deep bacterial reservoirs, and our data offer evidence that such penetration has occurred.

3.7 CapFuran can significantly reduce the burden of chronic infection in a human organoid model with a better cytoxicity profile than the FDA-approved free drug

We assessed the levels of cytotoxicity induced by various treatments and doses in the human urothelial organoid model by detecting the quantity of released lactate dehydrogenase (LDH), an intracellular protein that is only released upon cell damage (**Figure 5a)**. The addition of culture medium alone resulted in no toxicity. The clinically used dose of 200 μg/ml of unencapsulated nitrofurantoin (an FDA-approved drug) caused a slight increase in toxicity (med=6.59%, 95% CI: 6.22, 6.98), but the equivalent dose of the drug encapsulated in CapFuran (2mg/ml) elicited a lower level (med=5.17%, 95% CI: 5.14, 5.38). A Kruskal-Wallis test confirmed a statistically significant difference existed between the level of cytotoxicity induced by these various treatments ($\chi^2(4) = 12.85$, $p = 0.012$). We observed a dose-related response in the level of cytotoxicity. These data confirm that the production of these microparticles and the encapsulation process using the PLGA polymer does not adversely affect the viability of cells in a human bladder organoid and presents with lower toxicity when compared with an equivalent drug dose.

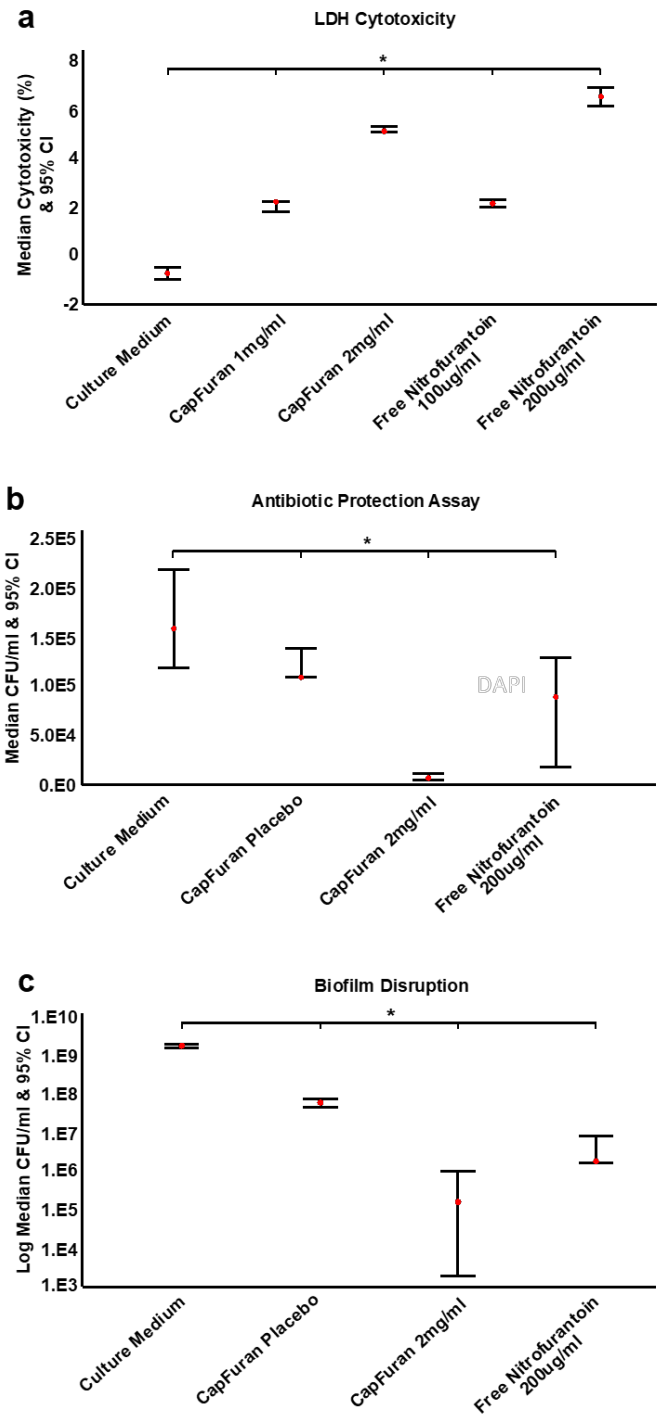

Figure 5: Safety and efficacy of CapFuran in the human organoid model and anti-biofilm activity
a) Human urothelial organoids were exposed to various CapFuran concentrations, nitrofurantoin concentrations and control (culture media only). Note that the active drug is 10% of the particle mass, so the actual drug doses are ten-fold lower. Cytotoxicity was calculated by measuring LDH release (N=3). Median and 95% plot showing the level of cytotoxicity (%) induced by these different treatments, p=0.012. **b)** Median and 95% CI of bacteria enumerated post lysis of urothelial organoid using the Antibiotic Protection Assay (N=3), p=0.037. **c)** Log Median and 95% confidence intervals of enumerated bacteria after mechanical disruption of biofilms that were treated overnight with either CapFuran, CapFuran-Placebo, media solution or free nitrofurantoin (n=3), p=.024. See Methods for statistical details.

We next used an antibiotic protection assay to inspect the ability of CapFuran's drug cargo to enter and kill protected bacterial reservoirs established within the human bladder organoid.

After infection with *E. faecalis* EFCIb under conditions in which intracellular reservoirs form [33], the extracellular space was sterilized with gentamicin and vancomycin, two antibiotics that cannot penetrate cells. Afterwards, the infected organoid was challenged with various treatments, and then lysed with detergent and plated to enumerate any residual bacterial growth "protected" inside the cell. These bacteria would have been resistant to levels achieved in the bladder by non-permeant or poorly permeant oral dosing regimes; this is important because intracellular reservoirs have been implicated in the propensity of UTI to recur in patients [11].

Figure 5b shows the median CFU/ml and 95% CI of bacteria enumerated in each treatment category after lysis of the bladder organoid. Bladder organoids treated with 200 mg/ml of CapFuran (equivalent to 200 μg/ml nitrofurantoin) exhibited a notable decrease in the number of intracellular bacteria (Med=$7x10^3$, 95% CI: $5x10^3$, $1.2x10^4$) compared with the CapFuran Placebo (Med=$1.1x10^5$, 95% $1.1x10^5$, $1.4x10^5$), and also a significant decrease compared with unencapsulated nitrofurantoin (Med=$9x10^4$, 95% $1.8x10^4$, $1.3x10^5$), suggesting that it is more effective at treating bacterial reservoirs. A Kruskal-Wallis test confirmed a statistically significant difference between these treatments ($\chi^2(3)=8.465$, $p=0.037$). Indeed, on inspection of the 95% confidence intervals, the effect of free nitrofurantoin was not statistically significantly different compared with that of cell culture media or CapFuran-Placebo conditions. It is not known whether *E. faecalis* internalised into bladder cells are metabolically active, but our data showing CapFuran-induced killing in this setting suggests that the bacteria do remain vulnerable to antibiotic treatment despite their intracellular setting. In the future, to render this modality useful against dormant intracellular bacteria, it should be possible to co-deliver factors capable of activating their metabolism, thereby inducing drug susceptibility.

In summary, by incorporating a drug into a microparticle system, it is possible to achieve higher local doses of antibiotics and greater efficacy than with the equivalent total dose of unencapsulated drug, with no adverse cytotoxicity. CapFuran was able to deliver active nitrofurantoin through the cell membrane and kill sequestered bacteria in a situation where the free drug did not perform well. Given that the majority of antibiotics are not cell permeant and even if permeant, would not be expected to accumulate to high concentrations within cells by free diffusion, this represents an important advance for high-dose, targeted intravesical therapy.

3.8 CapFuran is more effective at treating *E. faecalis* biofilms than is unencapsulated nitrofurantoin

Biofilms are protected by a polymeric extracellular matrix assembly that hinders antibiotic penetration; what's more, dormant bacteria within with biofilm are intrinsically antibiotic-resistant, as such drugs normally target aspects of active bacterial metabolism. One key anti-biofilm effect of encapsulated drugs is thought to be their ability to disrupt the biofilm architecture [43]. As *E. faecalis* readily forms biofilms, and these communities play a very important role in catheter-associated UTI [38], we wanted to test how CapFuran performed against them. Thus, we treated *E. faecalis* EFCIb biofilms grown *in vitro* with CapFuran and various control treatments overnight. Subsequently, the biofilms were washed and then mechanically disrupted before the supernatant was plated to assess the impact of the treatment on bacteria residing within the biofilm.

As shown in **Figure 5c**, CapFuran induced a 1.06 log ($1.7x10^6$ CFU) decrease in median CFU counts compared with free nitrofurantoin (CapFuran: Med= $1.65x10^5$, 95% CI: $1.9x10^3$, $1.05x10^6$; nitrofurantoin: Med=$1.9x10^6$, 95% CI: $1.7x10^6$, $8.5x10^6$). A Kruskal-Wallis test showed there to be a statistically significant difference in anti-biofilm properties exhibited by these different treatments ($\chi^2(3)=9.409$, p=.024). This result suggests that CapFuran has the ability to kill bacteria in biofilms. The detailed mechanism(s) will require further study in the future as there are mixed results in the literature regarding the impact of encapsulated antibiotics on biofilms that warrant further investigation [44, 45]. Supporting the idea that the capsules might be able to disrupt the polymeric matrix, however, CapFuran-Placebo was also seen to have a modest effect on the biofilm, resulting in fewer CFU/ml than biofilms treated with media solution alone (CapFuran-Placebo: Med= $6.5x10^7$, 95% CI: $5x10^7$, $8x10^7$; Culture Medium: Med=$1.975x10^9$, 95% CI: $1.75x10^9$, $2.2x10^9$). It is possible that CapFuran's anti-biofilm activity might also be relevant for its ability to kill intracellular bacteria, as studies have shown that, for example, uropathogenic *E. coli* forms biofilm-like communities when internalized within cells in a mouse model [11].

4. Conclusions

A fundamental problem in treatment of recurrent or chronic UTIs lies in the fact that oral doses are ineffective, requiring extended or often-repeated regimens. Most UTI drugs are now off-patent, and there has been a very substantial reduction in the development of new antibiotics. This vacuum of new treatment options means patients are poorly or incompletely treated and allows the risk of increasing numbers of antibiotic-resistant bacteria emerging, thereby exacerbating an already alarming global public-health crisis.

Our study used an advanced human bladder model to demonstrate that benchtop-produced CapFuran is safe and effective. We used this human model system because the mouse model of UTI has a number of drawbacks, whereas the organoid has been shown previously to give results concordant to patient data [33]. Our work demonstrates the ability of the electrospraying process to load an antibiotic into a porous polymeric microparticle that can enable cargo penetration through multiple layers of a human bladder organoid and effectively reduce the intracellular bacteria burden without undue toxicity. The approach was also shown to be more effective than drug alone against biofilms. By employing an intravesical approach using a urinary catheter, a simple procedure which can be carried out in the outpatient setting, highly localised doses could be introduced directly into the bladder whilst eliminating exposure of antibiotics to the gut microbiome and commensals in other niches. This would circumvent the current problems faced with treating recalcitrant UTI via long-term systemic antibiotics and would also eliminate the significant side effects that occur through oral ingestion of antibiotics.

Among the various controlled-release polymer technologies, PLGA has had the greatest clinical impact with a number of FDA approved medicines. Given that nitrofurantoin has already met regulatory approval, it can be assumed that the production of the CapFuran microparticles via "route-change" would face a streamlined regulatory approval for clinical trials. With chronic UTI as proof-of-principle, this method of producing microparticles might also be of more broad utility for clinical indications, including oncology and gene therapy, where robust and reliable intracellular delivery of small molecular drugs, proteins or nucleic acids would be useful.

5. Acknowledgements

We thank Caroline Pellet-Many, Ketevan Palishvili and Hannah Vickers for expert technical assistance, and members of our laboratories for helpful discussion. We further thank Scott Hultgren's lab for kindly providing the UTI89 strain.

6. Funding sources, disclosures and competing interests

This work was partially supported by AtoCap Ltd., a spin-off biotechnology company from University College London, and also received funding support from two anonymous philanthropic donations to the UCL team. The salary of DD was paid by the National Health Service as part of a clinical traineeship programme. ES and ME are non-executive directors of AtoCap Ltd. ES, ME, WKL and JLR are co-inventors on a patent (PCT/GB2019/050152) that has been filed in relation to the formulation described in the paper and licensed to AtoCap Ltd from University College London. This does not alter the authors' adherence to all the journal policies on ethics in publishing or sharing of data and materials.

7. Data availability statement

The processed data required to reproduce these findings cannot be shared at this time due to technical or time limitations.

8. References

1. O'Neill, J. *Tackling Drug Resistant Infections Globally: Final Report and Recommendations*. 2016; Available from: https://amr-review.org/sites/default/files/160525_Final%20paper_with%20cover.pdf.
2. Foxman, B., *Urinary tract infection syndromes: occurrence, recurrence, bacteriology, risk factors, and disease burden.* Infect Dis Clin North Am, 2014. **28**(1): p. 1-13.
3. Foxman, B. and P. Brown, *Epidemiology of urinary tract infections: transmission and risk factors, incidence, and costs.* Infect Dis Clin North Am, 2003. **17**(2): p. 227-41.
4. Harding, G.K. and A.R. Ronald, *The management of urinary infections: what have we learned in the past decade?* Int J Antimicrob Agents, 1994. **4**(2): p. 83-8.
5. Irwin, D.E., et al., *Worldwide prevalence estimates of lower urinary tract symptoms, overactive bladder, urinary incontinence and bladder outlet obstruction.* BJU Int, 2011. **108**(7): p. 1132-8.
6. Laupland, K.B., et al., *Population-based laboratory surveillance for tribe Proteeae isolates in a large Canadian health region.* Clin Microbiol Infect, 2007. **13**(7): p. 683-8.
7. Nicolle, L.E., *Urinary tract infections in the elderly.* Clin Geriatr Med, 2009. **25**(3): p. 423-36.
8. Wolfe, A.J., et al., *Evidence of uncultivated bacteria in the adult female bladder.* J Clin Microbiol, 2012. **50**(4): p. 1376-83.

9. Khasriya, R., et al., *Spectrum of bacterial colonization associated with urothelial cells from patients with chronic lower urinary tract symptoms.* J Clin Microbiol, 2013. **51**(7): p. 2054-62.
10. Coyne, K.S., et al., *Economic burden of urgency urinary incontinence in the United States: a systematic review.* J Manag Care Pharm, 2014. **20**(2): p. 130-40.
11. Hunstad, D.A. and S.S. Justice, *Intracellular lifestyles and immune evasion strategies of uropathogenic Escherichia coli.* Annu Rev Microbiol, 2010. **64**(May): p. 203-21.
12. Horsley, H., et al., *Enterococcus faecalis subverts and invades the host urothelium in patients with chronic urinary tract infection.* PLoS One, 2013. **8**(12): p. e83637.
13. De Nisco, N.J., et al., *Direct Detection of Tissue-Resident Bacteria and Chronic Inflammation in the Bladder Wall of Postmenopausal Women with Recurrent Urinary Tract Infection.* J Mol Biol, 2019. **431**(21): p. 4368-4379.
14. Tenke, P., et al., *Update on biofilm infections in the urinary tract.* World J Urol, 2012. **30**(1): p. 51-7.
15. Wood, T.K., S.J. Knabel, and B.W. Kwan, *Bacterial persister cell formation and dormancy.* Appl Environ Microbiol, 2013. **79**(23): p. 7116-21.
16. Lewis, K., *Multidrug tolerance of biofilms and persister cells.* Curr Top Microbiol Immunol, 2008. **322**: p. 107-31.
17. Fisher, R.A., B. Gollan, and S. Helaine, *Persistent bacterial infections and persister cells.* Nat Rev Microbiol, 2017. **15**(8): p. 453-464.
18. Stamm, W.E. and T.M. Hooton, *Management of urinary tract infections in adults.* N Engl J Med, 1993. **329**(18): p. 1328-34.
19. Chen, Y.H., W.C. Ko, and P.R. Hsueh, *Emerging resistance problems and future perspectives in pharmacotherapy for complicated urinary tract infections.* Expert Opin Pharmacother, 2013. **14**(5): p. 587-96.
20. Gupta, K. and N. Bhadelia, *Management of urinary tract infections from multidrug-resistant organisms.* Infect Dis Clin North Am, 2014. **28**(1): p. 49-59.
21. Taneja, N., et al., *Occurrence of ESBL & Amp-C beta-lactamases & susceptibility to newer antimicrobial agents in complicated UTI.* Indian J Med Res, 2008. **127**(1): p. 85-8.
22. NICE, *UTI (recurrent): antimicrobial prescribing*, in *NG112*. 2018.
23. Swamy, S.A.-O., et al., *Recalcitrant chronic bladder pain and recurrent cystitis but negative urinalysis: What should we do?* Int Urogynecol J, 2018. **29**: p. 1035-1043.
24. Zacche, M.M., S. Srikrishna, and L. Cardozo, *Novel targeted bladder drug-delivery systems: a review.* Res Rep Urol, 2015. **7**: p. 169-78.
25. O'Brien Vp Fau - Hannan, T.J., et al., *Drug and Vaccine Development for the Treatment and Prevention of Urinary Tract Infections.* Microbiology Spectrum, 2016. **4**(1).
26. Horsley, H., et al., *Ultrasound-activated microbubbles as a novel intracellular drug delivery system for urinary tract infection.* J Control Release, 2019. **301**: p. 166-175.
27. Pareta, R. and M.J. Edirisinghe, *A novel method for the preparation of biodegradable microspheres for protein drug delivery.* J R Soc Interface, 2006. **3**(9): p. 573-82.
28. Enayati, M., et al., *Preparation of polymeric carriers for drug delivery with different shape and size using an electric jet.* Current Pharmaceutical Biotechnology, 2009. **10**: p. 600-608.

29. Chang, M.W., E. Stride, and M. Edirisinghe, *Controlling the thickness of hollow polymeric microspheres prepared by electrohydrodynamic atomization.* J R Soc Interface, 2010. **7 Suppl 4**: p. S451-60.
30. Labbaf, S., et al., *Preparation of multicompartment sub-micron particles using a triple-needle electrohydrodynamic device.* Journal of Colloid and Interface Science, 2013. **409**: p. 245-54.
31. Schindelin, J., et al., *The ImageJ ecosystem: An open platform for biomedical image analysis.* Mol Reprod Dev, 2015. **82**(7-8): p. 518-29.
32. Labbaf, S., et al., *An encapsulated drug delivery system for recalcitrant urinary tract infection.* J R Soc Interface, 2013. **10**(89): p. 20130747.
33. Horsley, H., et al., *A urine-dependent human urothelial organoid offers a potential alternative to rodent models of infection.* Sci Rep, 2018. **8**(1): p. 1238.
34. Fau, N.M., et al., *The determination of lactic dehydrogenase with a tetrazolium salt.* Anal Biochem, 1960 **1**: p. 317-26.
35. Decker, T. and M.L. Lohmann-Matthes, *A quick and simple method for the quantitation of lactate dehydrogenase release in measurements of cellular cytotoxicity and tumor necrosis factor (TNF) activity.* J Immunol Methods, 1988. **115**(1): p. 61-9.
36. Enayati, M., et al., *Size mapping of electric field-assisted production of polycaprolactone particles.* J R Soc Interface, 2010. **7 Suppl 4**: p. S393-402.
37. Foxman, B., *The epidemiology of urinary tract infection.* Nat Rev Urol, 2010. **7**(12): p. 653-60.
38. Nicolle, L.E., *Catheter-related urinary tract infection.* Drugs Aging, 2005. **22**(8): p. 627-39.
39. Khandelwal, P., S.N. Abraham, and G. Apodaca, *Cell biology and physiology of the uroepithelium.* Am J Physiol Renal Physiol, 2009. **297**(6): p. F1477-501.
40. Eto, D.S. and M.A. Mulvey, *Flushing bacteria out of the bladder.* Nature Medicine, 2007. **13**: p. 531-2.
41. Perel, P., et al., *Comparison of treatment effects between animal experiments and clinical trials: systematic review.* BMJ, 2007. **334**: p. 197.
42. Wu, X.R., et al., *Uroplakins in urothelial biology, function, and disease.* Kidney Int, 2009. **75**(11): p. 1153-1165.
43. Dos Santos Ramos, M.A., et al., *Nanotechnology-based drug delivery systems for control of microbial biofilms: a review.* Int J Nanomedicine, 2018. **13**: p. 1179-1213.
44. Santos Ferreira, I., et al., *Encapsulation in Polymeric Microparticles Improves Daptomycin Activity Against Mature Staphylococci Biofilms-a Thermal and Imaging Study.* AAPS PharmSciTech, 2018. **19**(4): p. 1625-1636.
45. Thomas, N., et al., *Efficacy of Poly-Lactic-Co-Glycolic Acid Micro- and Nanoparticles of Ciprofloxacin Against Bacterial Biofilms.* J Pharm Sci, 2016. **105**(10): p. 3115-3122.

Fig 1

Click here to download high resolution image

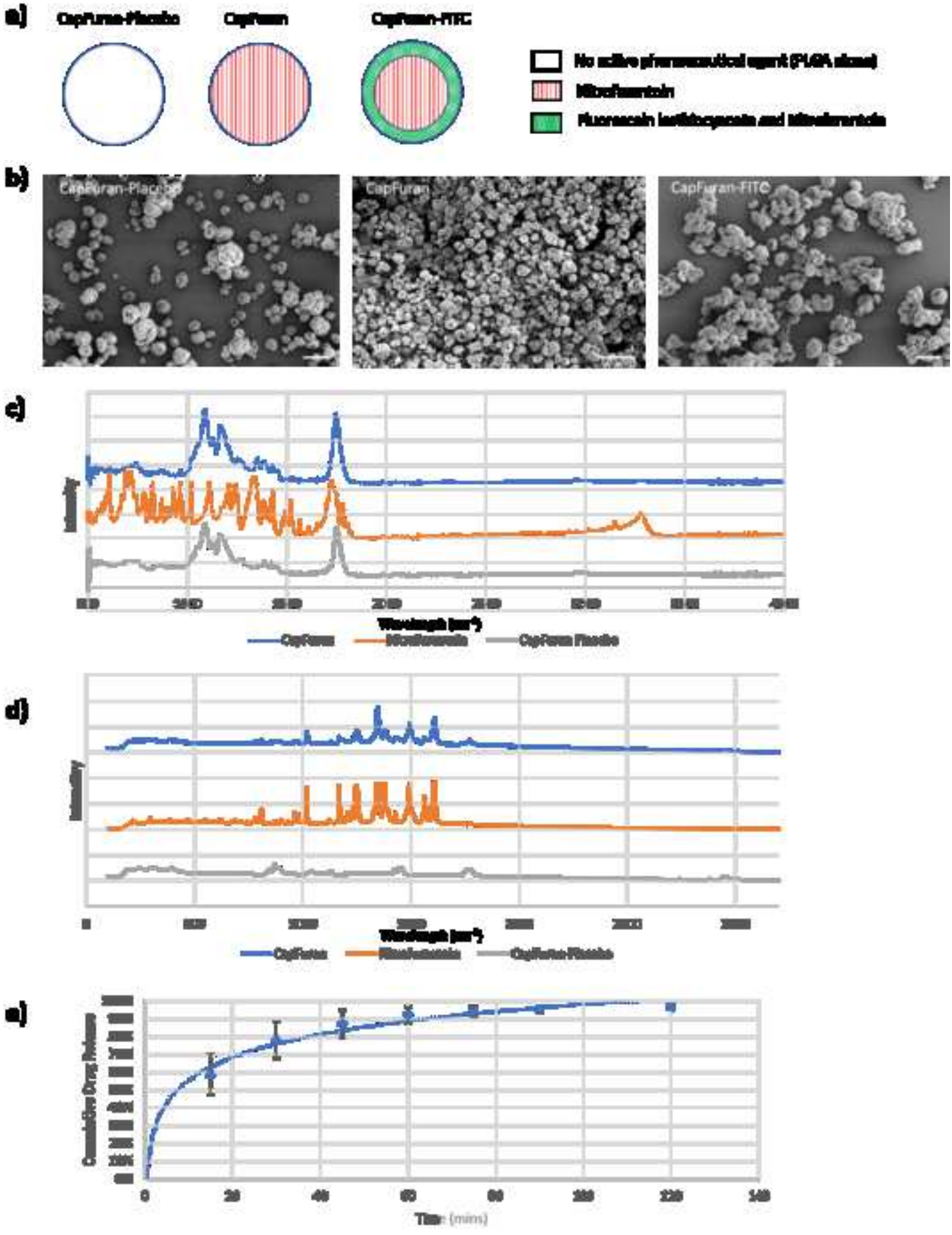

Fig 2

Click here to download high resolution image

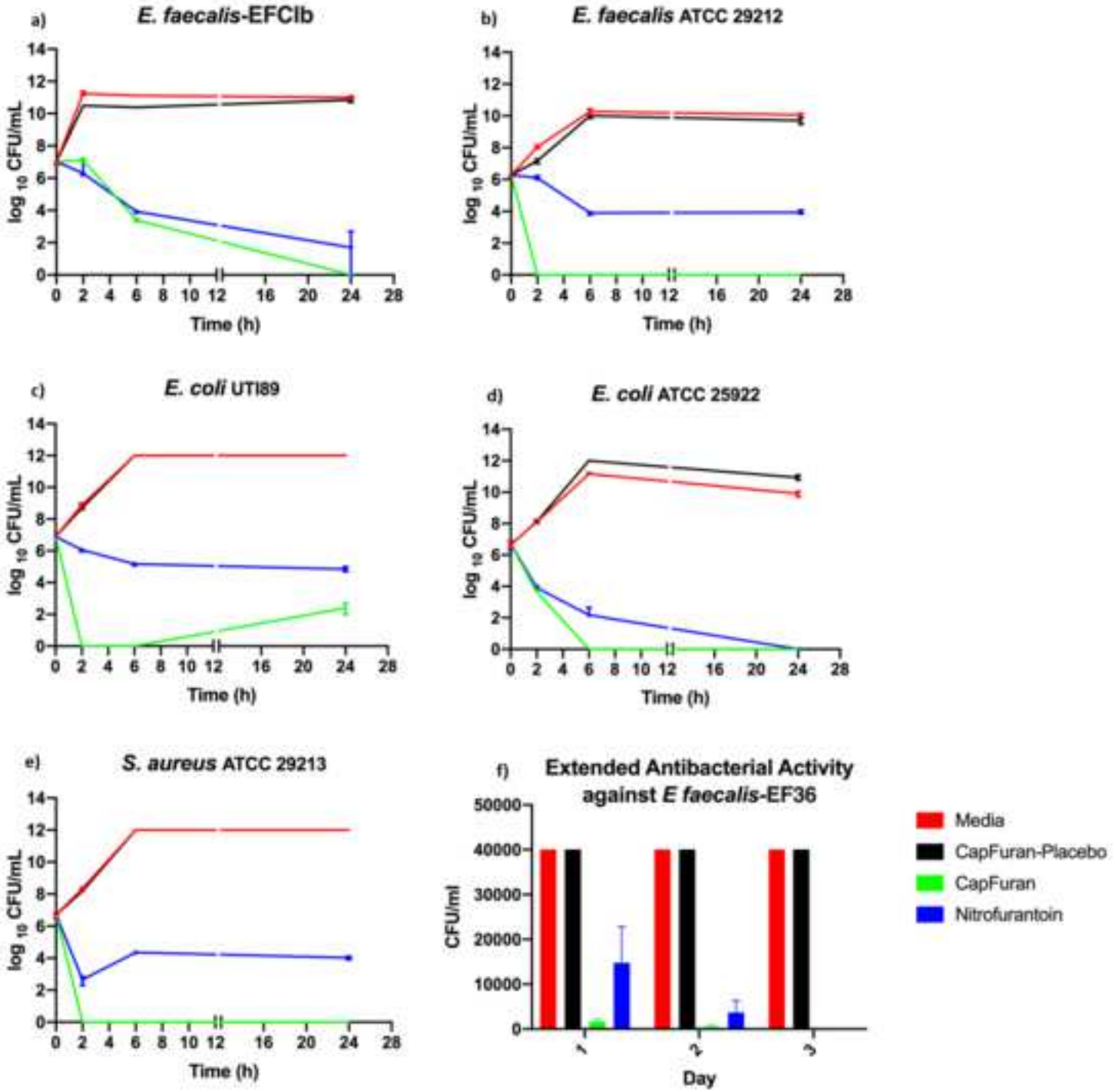

Fig 3

Click here to download high resolution image

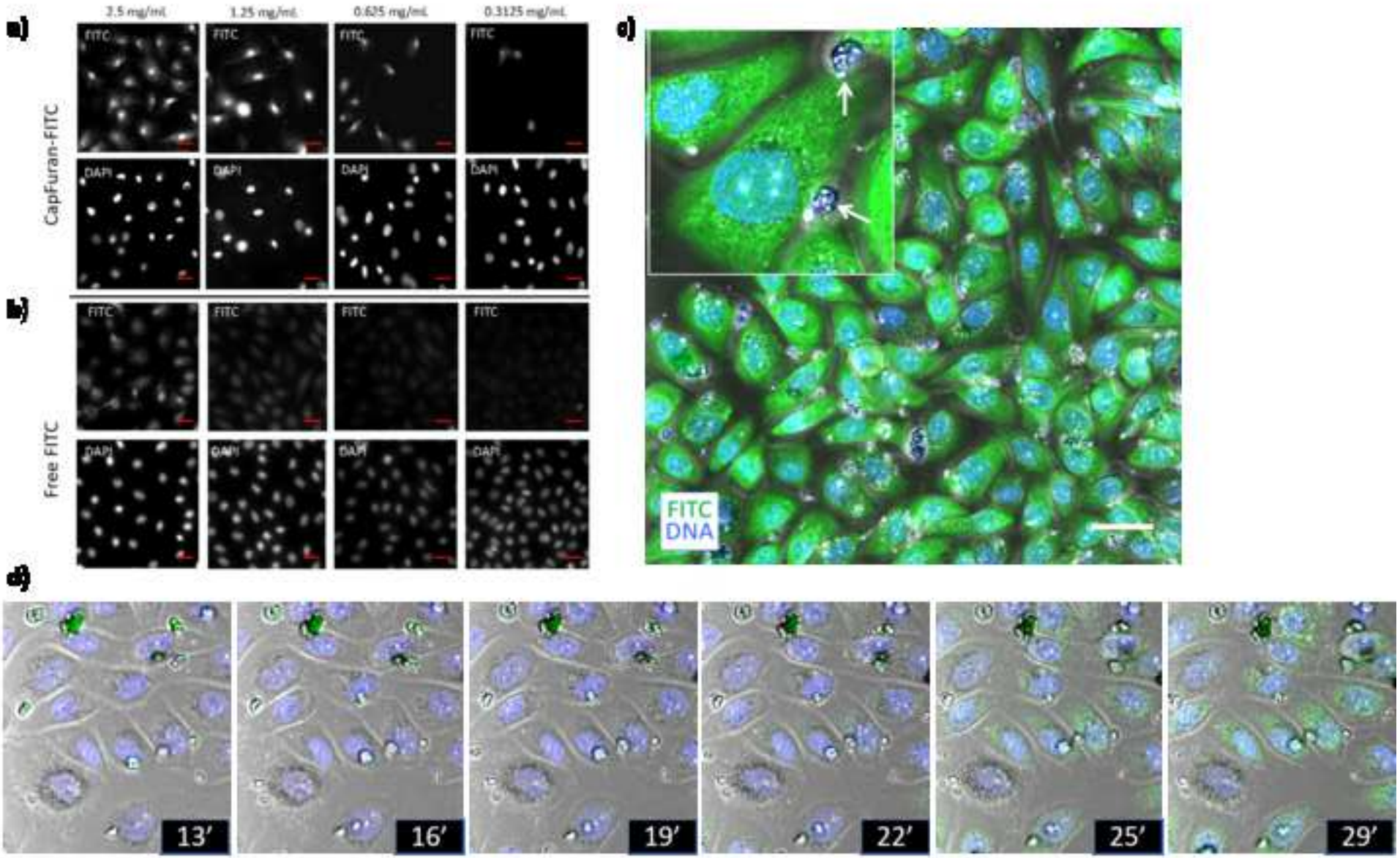

Fig 4

Click here to download high resolution image

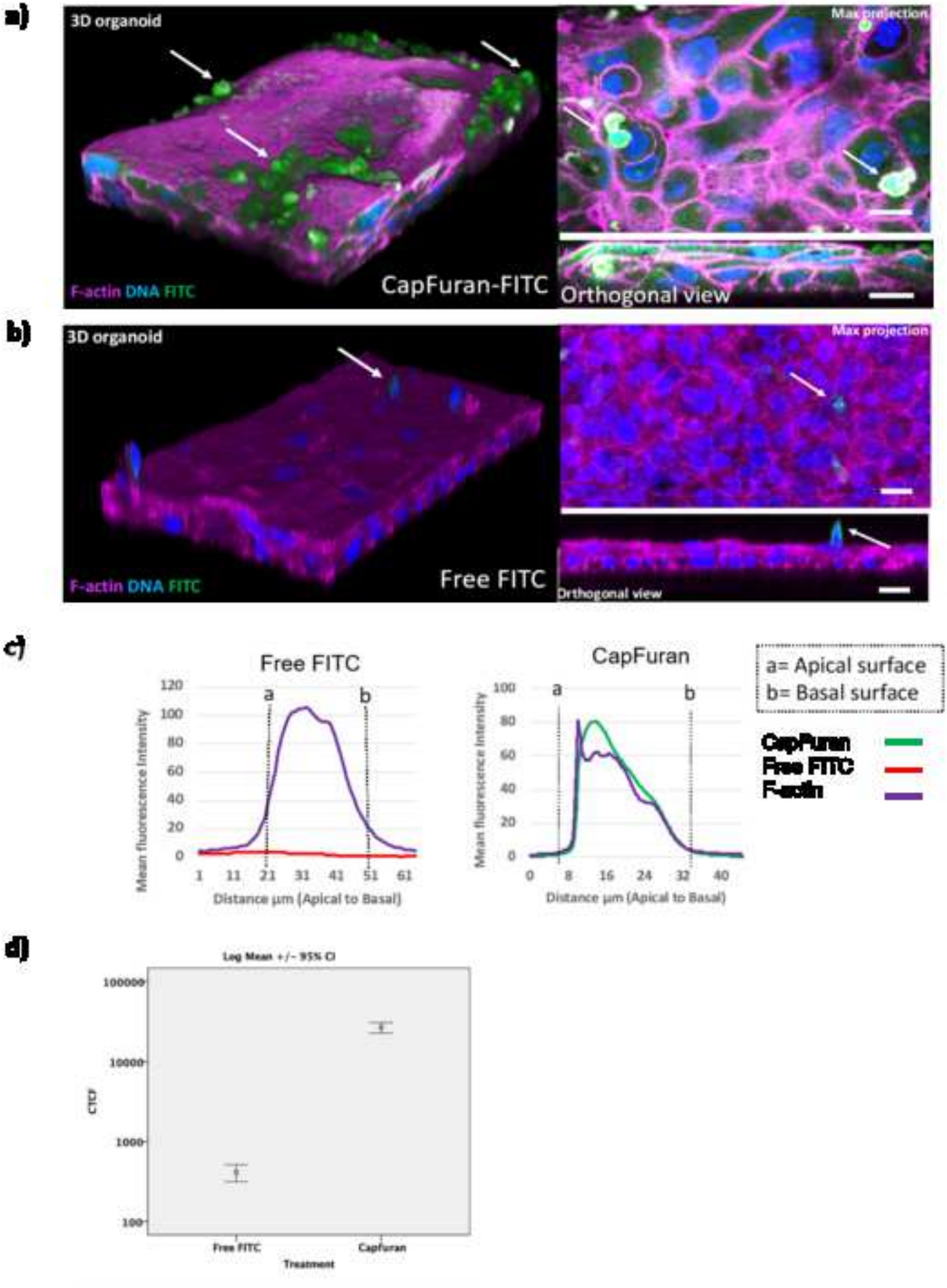

Fig 5

Click here to download high resolution image

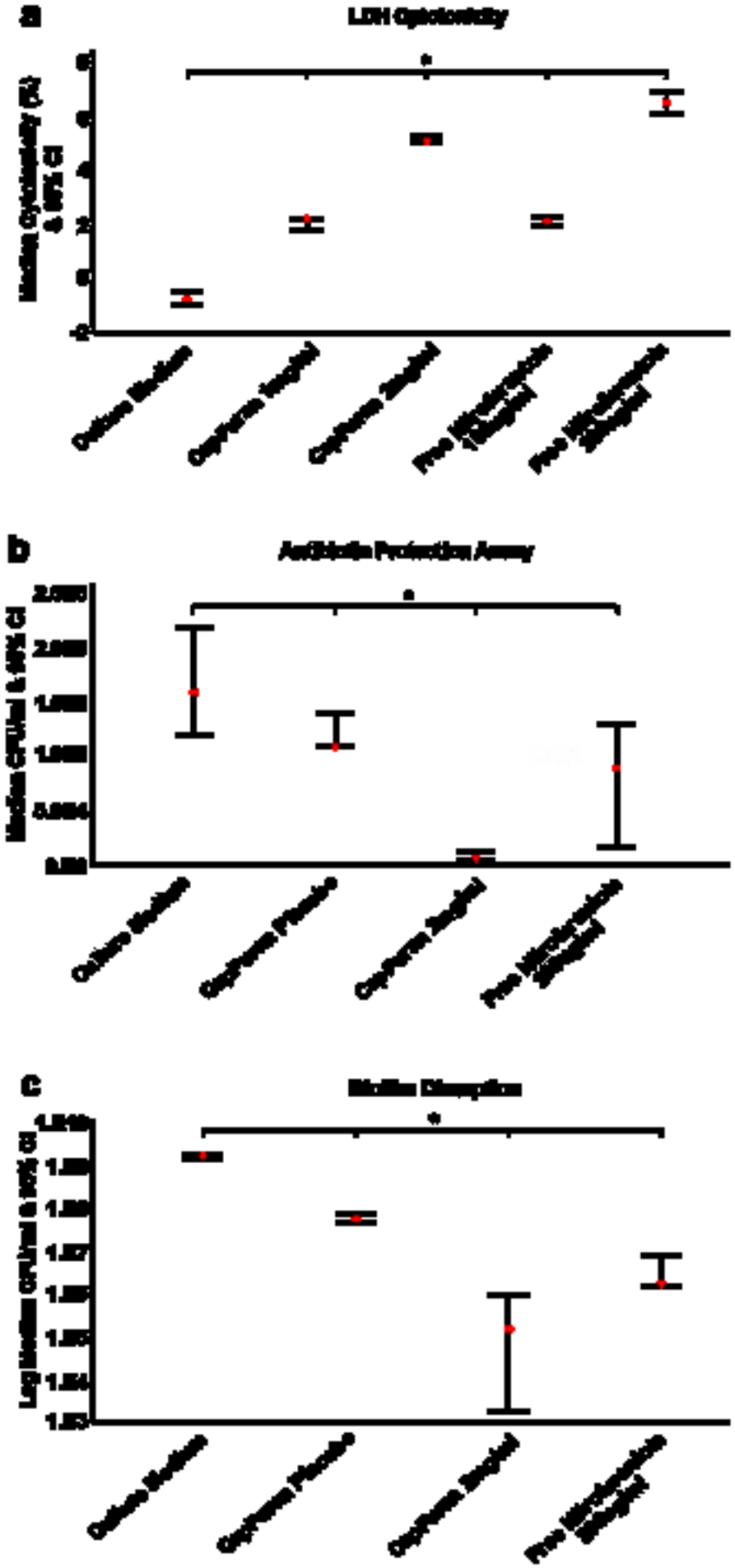

marked up version of manuscript showing changes

Click here to download Supplementary Material: Capsule Paper Final JCR Revised marked up.docx

Video

Click here to download Video: capfuran gif.gif

***Credit Author Statement**

Wai K. Lau: Investigation, Writing - Original Draft, Visualisation
Dhanuson Dharmasena: Investigation, Writing - Original Draft, Visualisation
Harry Horsley: Investigation, Writing - Original Draft, Visualisation
Nazila V. Jafari: Investigation, Writing - Original Draft, Visualisation
James Malone-Lee: Conceptualization, Methodology, Resources
Eleanor Stride: Conceptualization, Methodology, Writing - Review & Editing, Funding acquisition, Project administration,
Mohan Edirisinghe: Conceptualization, Methodology, Writing - Review & Editing, Supervision, Funding acquisition, Project administration,
Jennifer L. Rohn: Conceptualization, Methodology, Writing - Review & Editing, Supervision, Project administration, Funding acquisition